

AN EMITTANCE MEASURING SYSTEM FOR HIGH-CURRENT HIGH-BRIGHTNESS

MULTI-BEAMLET MULTI-SPECIES HEAVY-ION BEAMS

T. Taylor, M.S. de Jong and W.L. Michel
Atomic Energy of Canada Limited, Chalk River Nuclear Laboratories,
Chalk River, Ontario, Canada K0J 1J0

Abstract

A two-slit emittance measuring system for high-current high-brightness multi-beamlet multi-species ion beams has been developed. High-density graphite has been used extensively on components exposed to the beam so that sputtering damage is minimized. A separator magnet mounted between the front slit and the back slit allows the emittances of the several species that comprise the beam to be measured simultaneously. The transmitted current is measured by a Faraday cup positioned behind the back slit. A personal computer controls stepping motors and also acquires and analyzes data from the Faraday cup. The data are transformed to facilitate the calculation of the emittances corresponding either to the individual beamlets of a multi-beamlet beam or to the individual species of a multi-species beam. Measurements will be presented to demonstrate the versatility of the system.

Introduction

A suitable emittance measuring system¹ is an essential tool of every ion source development program. The present paper describes the emittance measuring unit (EMU) that has evolved at Chalk River as an integral part of a program to develop high-current high-brightness ion sources. The special considerations involved in handling beams of hundreds of milliamps with energies of tens of kilovolts are emphasized. In addition, the protection of sensitive electronics against the effects of vacuum sparking is addressed. Also, a novel technique for analyzing the complex phase-space distributions produced by ion sources with several apertures or generated when beams of several ion species are momentum dispersed will be introduced.

Mechanical System

The Chalk River EMU, shown in Fig. 1, is based on the "two-slit method"¹. The first (or X) slit is embedded in a water-cooled beam stop that intercepts most of the beam. The second (or X') slit is mounted in front of a Faraday cup that collects the transmitted ions. The X'-slit/Faraday cup assembly traverses the beam on a carriage which is in turn mounted on a second carriage that also carries the X-slit/beam stop assembly across the beam. Both carriages are driven by vacuum stepper motors. The slits are 0.05 mm wide by 6.35 mm high and are separated by 320 mm. A small electromagnet mounted behind the X-slit separates multi-species beams.

The usual design concepts for high-power beam stops emphasize heat dissipation. Typically, an array of copper swirl tubes is mounted at an oblique angle with respect to the beam so as to distribute the thermal load. Unfortunately, at the beam energies of interest here, the sputtering yield is exceptionally high for copper at oblique angles of incidence, especially for heavy ions.² On the other hand, graphite at normal incidence is unusually sputter resistant. Hence, the beam stop in the present system consists of a water-cooled copper block mounted normal to the beam with a high-density graphite plate brazed to the front face using a titanium-copper-silver alloy. In addition, the X-slit is fabricated entirely from high-density graphite. The graphite components have proved to be very durable.

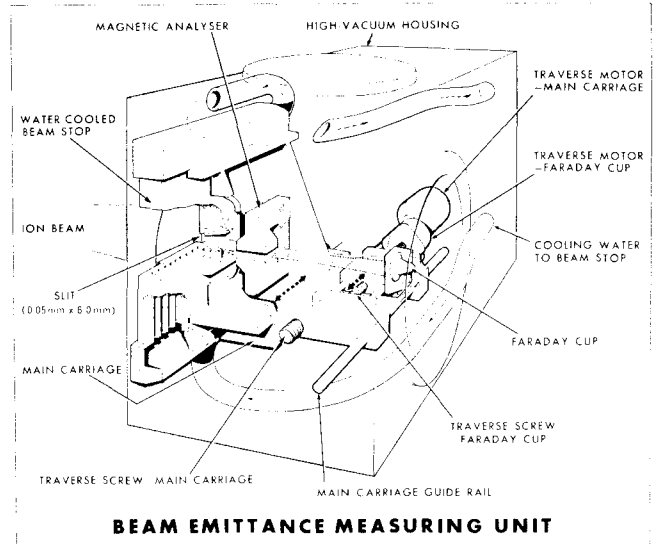


Fig. 1: The Chalk River emittance measuring unit.

Control and Data Acquisition

The emittance measurement system is fully automated. A host computer manages two subsystems: the first controls the motion of the two carriages while the second acquires the data from the Faraday cup. A block diagram of this control and data acquisition system is presented as Fig. 2.

The host computer is an IBM-XT with 640 kilobytes of RAM, a 10 megabyte hard disk drive, a 320 kilobyte floppy disk drive and a dot matrix printer. Communication with the control and data acquisition subsystems is via RS-232 serial links through the COM1: and COM2: ports. The operator uses the host computer to send command strings to the subsystems and monitor their responses. A real-time display of the raw data is

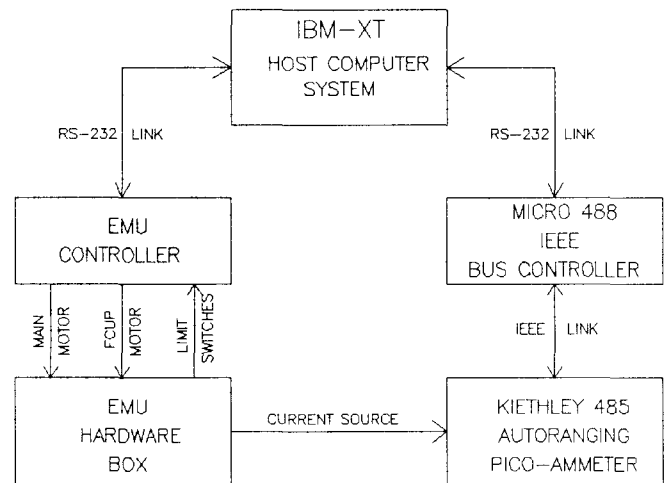


Fig. 2: The control and data acquisition system.

generated while an emittance measurement is in progress. The host program was written and compiled using the MICROSOFT QuickBASIC compiler.

An INTEL 8085 based microprocessor controls the motion of the SLO-SYN stepper motors via a CY6215 motor-control chip. The controller accepts ASCII coded instructions from the IBM-XT, validates them and passes them on to the motor-control chip for execution. It also processes interrupts such as high- and low-limit indications. Carriage positions, limit status, etc., are reported back to the host computer in ASCII code. The control software is contained on a 32 kilobyte EPROM.

The data acquisition system is built around a Kiethly 485 autoranging picoammeter. The picoammeter communicates with the IBM-XT via a MICRO 488 IEEE bus controller. Whenever a reading is required the host computer sends an ASCII coded instruction to the picoammeter and receives the data back in ASCII format.

An EMU must operate in an exceptionally harsh environment with periodic ion-source arc downs radiating enormous power. For this reason, great care was taken in shielding every motor and signal cable, all electronic equipment was fully enclosed, filters were installed on all ac-power lines and MOVs on all motor and signal cables. Finally, the RS-232 links with the host computer were optically isolated. The entire control and data acquisition system has been demonstrated to be very robust.

Data Analysis

A standard two-slit emittance measurement yields¹ $\rho_{ij}(X_i, X'_i)$, a sampling of the beam's X-X' transverse phase-space density. The slits are assumed to be long enough to integrate over the beam density in Y-Y' phase space. Usually there are strong X-X' correlations in $\rho(X, X')$ making the determination of the emittances of the individual beamlets or the separated species difficult. These correlations can be removed by using the coordinate transformation, R(u),

$$\begin{pmatrix} X \\ X' \end{pmatrix} = R(u) \begin{pmatrix} X \\ X' \end{pmatrix} \quad \text{where } R(u) = \begin{pmatrix} 1 & 0 \\ u & 1 \end{pmatrix} \quad (1)$$

to generate the distribution $\tilde{\rho}(x, x')$. The linear transformation preserves the emittance of the total beam, as well as the beamlet/species emittances, since $\det(R)=1$. The transformation parameter, u, is selected to minimize the x-x' correlation of the beamlets/species as is shown in Fig. 3. $\tilde{\rho}(x, x')$ can then be interpolated on a uniform grid for further calculations.

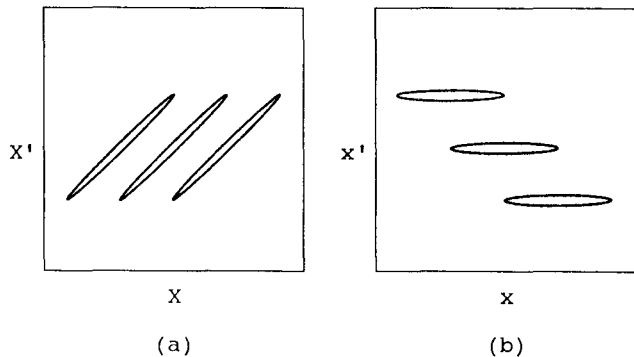


Fig 3: A contour plot of the phase-space density before, (a), and after, (b), the transformation specified by Eq. 1.

A rectangular subregion, D, of phase space containing the beamlet of interest is selected, and the rms emittance in the subregion is evaluated. The calculation is performed by computing the total current, I_D , and the first and second moments of the distribution in D:

$$\begin{aligned} I_D &= \iint_D \tilde{\rho}(x, x') dx dx' \\ \langle x \rangle &= \iint_D x \tilde{\rho}(x, x') dx dx' / I_D \\ \langle x' \rangle &= \iint_D x' \tilde{\rho}(x, x') dx dx' / I_D \\ \langle x^2 \rangle &= \iint_D x^2 \tilde{\rho}(x, x') dx dx' / I_D \\ \langle x'^2 \rangle &= \iint_D x'^2 \tilde{\rho}(x, x') dx dx' / I_D \\ \langle xx' \rangle &= \iint_D xx' \tilde{\rho}(x, x') dx dx' / I_D \end{aligned} \quad (2)$$

Now, let:

$$\begin{aligned} \overline{x^2} &= \langle x^2 \rangle - \langle x \rangle^2 \\ \overline{x'^2} &= \langle x'^2 \rangle - \langle x' \rangle^2 \\ \overline{xx'} &= \langle xx' \rangle - \langle x \rangle \langle x' \rangle \end{aligned} \quad (3)$$

Thus the beamlet/species having a total current I_D , mean position $\langle x \rangle$ and direction $\langle x' \rangle$, is described by the mean-square sigma matrix³:

$$\tilde{\sigma}_{ms} = \begin{pmatrix} \overline{x^2} & \overline{xx'} \\ \overline{xx'} & \overline{x'^2} \end{pmatrix} \quad (4)$$

and has an rms emittance given by:

$$\epsilon_{rms} = \left[\overline{x^2} \overline{x'^2} - (\overline{xx'})^2 \right]^{1/2} \quad (5)$$

To recover the sigma matrix in the original coordinate system, σ_{ms} , the inverse transformation of (1) is applied giving:

$$\sigma_{ms} = R(-u) \tilde{\sigma}_{ms} R^T(-u) \quad (6)$$

The brightness, normalized emittance, apparent beam waist and beam divergence are then easily calculated. The analysis can be performed on each beamlet/species or on the entire beam.

The calculations are performed on the IBM-XT with a FORTRAN program that first removes a linear background and smooths noise from the raw data.

Demonstration

Figure 4 shows a contour plot of the transformed phase-space density for a 30 kV, 25 mA Ar⁺ beam generated by a three-beamlet duoPIGatron. The rms emittances of the outer beamlets are only three-quarters of the rms emittance of the centre beamlet. This is probably attributable to non-uniformities in the distribution of the ion source plasma.

The transformed phase-space density for a 30 kV, 28 mA hydrogen beam produced by a single-aperture duoPIGatron is shown in Figure 5. The magnet was energized so that

the H_1^+ , H_2^+ and H_3^+ ions generate separate peaks. The rms emittances of the H_1^+ and H_3^+ are about twice the rms emittance of the H_2^+ . This may indicate that the processes that generate the H_2^+ have spatial distributions different from those that create the H_1^+ and H_3^+ .

These data are intended only to give an indication of the capabilities of the system. More extensive results will be published elsewhere.

Conclusions

A two-slit EMU has been developed for analyzing high-current high-brightness multi-beamlet multi-species ion beams. The system has proven to be very serviceable and promises to provide useful information on the processes involved in the generation and the extraction of ion beams from plasma sources.

The authors would like to acknowledge the pioneering contributions of J.H. Ormrod, J.G. Plato and M.R. Shubaly to the development of this system. The assistance of E.C. Douglas with the mechanical design, B.H. Smith with the development of the electronics and J.S.C. Wills in the data collection were very much appreciated.

References

1. C. LeJeune and J. Aubert, in "Applied Charged Particle Optics", ed. A. Septier (Academic Press, NY, 1980) pp. 159-259.
2. H.H. Anderson and H.L. Bay, in "Sputtering by Particle Bombardment I: Physical Sputtering of Single-Element Solids", ed. R. Behrisch (Springer-Verlag, Berlin, 1981) pp. 145-218.
3. F.J. Sacherer, IEEE Trans. Nucl. Sci. NS-18 (1971) 1105.

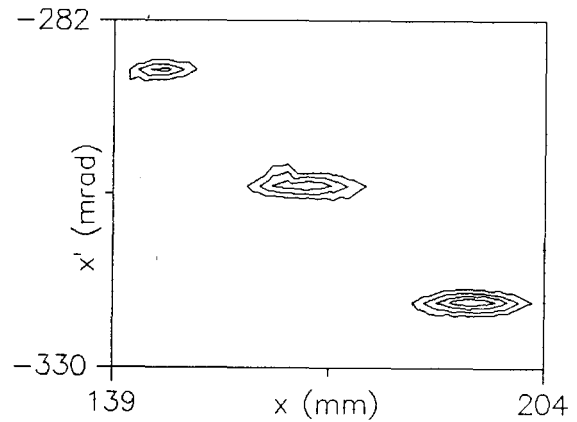


Fig. 4: A contour plot of the transformed phase-space density for a three-beamlet Ar^+ beam.

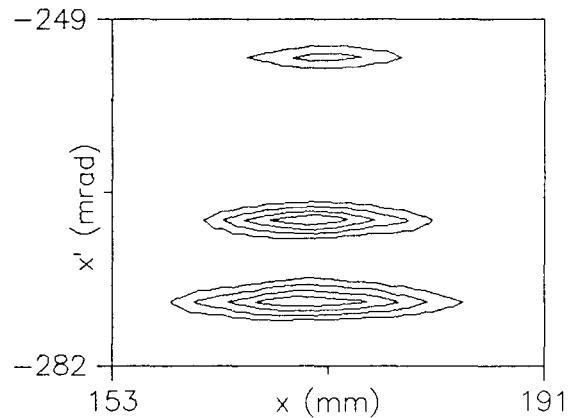


Fig. 5: A contour plot of the transformed phase-space density for a separated hydrogen beam.